Journal of Critical Reviews
ISSN- 2394-5125 Vol 7, Issue 2, 2020

Review Article

# A NOVEL CONVOLUTIONAL AUTOENCODERS BASED MULTILEVEL DENOISING FRAMEWORK FOR MEDICAL IMAGE DATA

[1]K.Kiran Kumar, [2]Dr.Rajasekar.B

[1] Research Scholar, Sathyabama Institute Of Science And Technology, Chennai, koya.kirankumar@gmail.com
[2]Associate Professor, Sathyabama Institute Of Science And Technology, Chennai,
rajasekar.ece@sathyabamauniversity.ac.in

*Received: 10.11.2019* *Revised: 15.12.2019* *Accepted: 16.01.2020*

**ABSTRACT**
Convolutional autoencoders based image denoising has emerged as a promising approach in medical imaging applications. Most of the traditional denoising methods such as Bayesian filter, non-linear median filter, wavelet based shearlet transform etc, are difficult to process medical images due to the existence of additive, multiplicative and Gaussian noise. Also, these models cannot resolve the issue of sparsity in the compressed medical images. To overcome these issues, a novelcompressive sensing based multilevel denoising technique is proposed to minimize the noise rate of medical images in the Convolution neural network(CNN) framework. This technique is implemented in convolutional autoencoders framework to reduce the noise in each deep network layer and to improve the quality of the images. This technique efficiently denoise the medical images using the inter, intra variance in the CNN framework. Experimental results demonstrated that the proposed framework has better PSNR and SSIM measures compared to the traditional state-of-the-art approaches.

***Keywords:***Denoising, deep learning, Compressive sensing, Medical data


DOI: http://dx.doi.org/10.31838/jcr.07.02.07

## INTRODUCTION

Image denoising methods are categorized as spatial domain, transform domain and dictionary learning based methods. Different algorithms have been proposed in the literature. In the following section, we describe briefly about these methods. Spatial domain methods attempt to utilize the correlation that exists in most natural images. It utilizes the similarities among either pixels or patches in an image [5]. Spatial domain filters can be categorized as local and nonlocal filters. In case of local filter, the pixel selection process depends only on spatial distance whereas in case of non-local filter, it depends only on the similarity [6-7].

Several edge based methods have been proposed in the literature to find the medical disease disease patterns, but the frequently accepted segmentation systems are edge based thresholding, which is used to clear noisy edges in bright conditions. Edge image thresholding directs to stray edges in the presence of noise where the actual edges are frequently missing . Stray edge problems can be cleared if the edge properties are decided with respect to the mutual neighbor, while the presence of edge based on the strength of edges in the near neighborhood. Region based segmentation approach which depends on the homogeneity measure to divide and merge regions in an image so as to broaden semantic or useful division in the processed image.In background detection process, the background is isolated from the foreground objects. Image thresholding is most often implemented in various applications of image segmentation [8]. It is quite complex task to get an optimal value of threshold. This threshold can affect system's performance to a great extent. Large numbers of failed recognitions are detected in case of high threshold value. System appears to be more sensitive with large numbers of medical disease images, when the threshold is very low. If there are very limited or no changes in features, static threshold value is used for evaluation. But the scenarios having more random changes require dynamic threshold. Dynamic threshold overcomes the problems of static threshold.

Histogram representation is often used for describing features in image reconstruction[4]. The histogram intersection match is defined in the following Equation.

$$D_i(H_1, H_2) = \frac{\sum_{k=1}^{K} \min(H_1(k), H_2(k))}{\sum_{k=1}^{K} H_2(k)}$$

The normalized histogram intersection method which minimizes the effect of the pixels in the edges or featurs in denoising process.

Recently, deep learning framework has been used to improve the performance of the image processing approaches such as feature extraction, classification, segmentation from medical images.Deep neural network (DNN) has the ability to classify the patterns using deep layer-wise architecture. Most of the commonly used deep neural network architecture include DNN and Convolution neural network(CNN) for image processing tasks. The autoencoder (AE)[1] is used to find the features from the image in each layer of deep neural network. Here, the performance of the AE is reduced due to the existence of noise in each layer of the training data. To solve this problem, the denoising autoencoder model is proposed in [2] to remove the noise from the input images. Traditionally,probabilistic graphical models are used to denoise the medical images using the directed acyclic graph and undirected graph mechanism. The undirected graph based model is used to find the entity feature extraction among the stratified random variables in image wavelet subbands.The hidden markov model is the well known undirected graph based model for image reconstruction process. But, the Markov Random Field (MRF) [2] model incorporates the spatial relationships among the graph nodes. So, an improvement to this MRF model is a Conditional Random Field (CRF) is applicable for edge based image reconstruction.

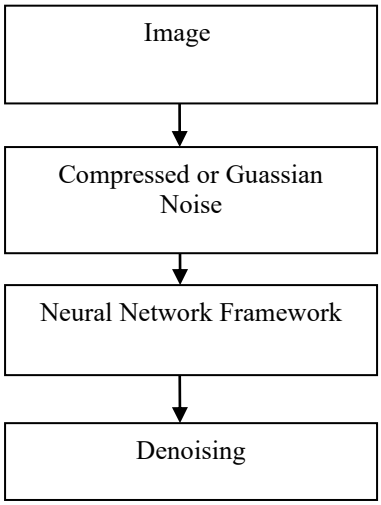


**Figure 1: Traditional Thresholding based image denoising**

In paper[3], authors proposed an empirical two-dimensional decomposition mode (BEMD) is performed in digital images. There are three-dimensional cubes showing BEMD's output which are well aligned with intuition and physical perception. In order to interpret the observed behaviors, the theoretical interpretation is supported by numerical experiments. This is usually due to errors in data transmission. It only has two possible meanings, a and b. Usually every likelihood is less than 0.1. Additionally, the defective pixels are set to the maximum or lowest value. This means that the image appears unchanged like "salt and pepper" pixels. For pepper noise the standard value is 0 on an 8-bit image, and 255 on salt noise. In general, salt and pepper noise is caused by pixel elements malfunction in camera sensors, memory faults, or digitisation errors[4]. If the image signal is digitally transmitted via a linear dispersive channel, it will otherwise interfere with symbols (ISI). Moreover, the presence of AWGN in a practical channel can not be ignored. The situation is therefore getting worse. A' 1' can be called 0' and vice versa because of ISI and AWGN. In these circumstances, pixel image values have changed to certain Random Impulse Noise (RVIN) signals. The fact that electromagnetic waves such asx-rays, visible lights and gamma rays have statistically determined their presence. The sources of x-rays and gamma-rays reveal a number of photons per unit of time[5]. These rays are pumped into the patient's body, into medicalx-rays and imagery for gamma rays from their source. Such sources fluctuate randomly with photons. The resulting image is random in time and space. This noise is also referred to as quantity or photon noise or shot noise. Poisson noise is a form of electronic noise when the finite number of particles that carry energy, such as electronic circuits or photons in optical systems, is small enough to cause observable statistical fluctuations. Initially, image is first marked and then interpolated. The denoising process, however, will kill the image edge structures and introduce devices. Meanwhile, edge preservation in denouncing and interpolating images is a critical issue. The authors suggest a directional denotion system, which inevitably provides a corresponding directional interpolator, to address these issues. Multi-visual image in a single LCD display, resize for displaying pixel strength and depth information. When used with L1 standard to generate the energy function that improves the seam carving algorithm, the combination of 2D images and depth mapping offers very precise inter and intra-object borders. The forward energy is expanded by virtual points to calculate the cost of seam insertion and a scale-invariant transformation (SIFT) approach is used to analyze the similarities between two images. In terms of the limitation, the system proposed only works best for small image resizing. Some retargeting methods other than seam carving can be used with the reverse concept. The authors also developed a technique to eliminate statistical traces of blocking objects left behind by algorithms for compression of images which divide the image into segments over time. Through a series of experiments the author has shown that anti-forensic techniques can eliminate forensically detectable traces of image compression without having a significant impact on image visual quality. [6] employed a simple Huffman coding technique to implement a lossless image compression and decompression process. This technique is easy to implement and less memory is required. The MATLAB platform used Huffman coding techniques to develop and implement a software algorithm to compress and decompress the given image. Some of these strategies are the methods of Area Rising (RG) and Active Contour (AC)[7]. In addition, with a few exceptions, the boundary evolution of the objects based on the edge detector might be prone to noise. Methods that focus on increasing areas are also noise-prone. AC-based approaches, on the other hand, could at least to some extent survive noise. All RG and AC methods rely heavily on initialization. While there are many changes to the AC method the demand for a more reliable object limit detection method remains high, particularly for medical images. The NMR theory includes quantum and classic mechanics involving the processing under external magnetic field of the proton (present in the human body). The core of the RIM is the use of the hydrogen nucleus abundance concentration in the form of water found in the human body. The H-atom protons are matched with the external field. Protons release their energy with the RF pulse, generating an electromagnetic signal captured by MRI receiver spools as shown in figure 2. These electromagnetic signals are stored in phase and frequency components. The Inverse Fourier raw data transformation produces 2 or3-dimensional image slices, also known as k-space. The reconstruction process from raw signal to picture space offers an additional choice for the generation of a specific 2D slice (3D) representation. Furthermore, the study showed that the type of noise in MR images is very different from the natural pictures. This occurs because of and combination of several specific noise sources. Therefore, it is very clear that the procedure used to denote the natural image can not function properly with medical images. Another inspiration was to study such noise and the technique for noise reduction.

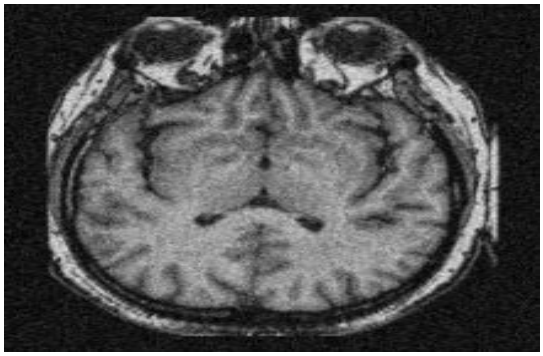

**Figure 2: Noisy MRI image**

Most of the MRI data are independent of edge detection methods and could not capture all edges. The edges that we seek create object boundaries that must be closed in nature. Closed limits are intended to regulate processes of denotation near borders where two distinct tissues interact. Otherwise, a type of tissue denouncement can influence / disturb a different type of border tissue. However, most of the methods suggested earlier[8] have difficulty finding such closed limits when placing borders. The magnitude of the coefficients varies according to the degree of decomposition of the wavelet. If all the rates are processed with a common threshold value, the image processed can be excessively smoothed to prevent sufficient information and to blur the image. In [9] proposed a superior performance, data-driven system and level-dependent methods to resolve the adaptive subband system, namely Bayes Shrinks, Oracle Shrinks, and Oracle thresholds. Both approaches remove D.L's proposed performance-safe retraction technique. As an adaptive and data-driven sub-banded framework. In [10], a special threshold methods for adaptive waving, such as Normal Shrink (NS) for image denoising Modified Bayes Shrink. They proposed a new wavelet based denoising method using the new thresholding function that eliminates the noise based on the shrinkage method.

Authors developed automatic focus and fusion image approach with the help of non-linear correlation [11].They introduced an advanced autofocus and fusion technique in order to improve the characteristics of the image along with reduced execution time. The above-mentioned autofocus approach has the responsibility to choose the best focused image in between stack of images gathered from various distances from the object. For every individual image in a particular stack, a vector is defined.

The vector includes different elements selected through spiral scanning of the image. The spectrum for free individual vector is evaluated with the help of fourier transform method. After that, nonlinear correlation must be implemented to the reference vector spectrum. For every individual image of stack, the relevant BFI is calculated. The complete process of fusion is performed along with a sub-group of images. It helps to evaluate the measure value close to the BFI ones. After that, the parabolic filter is implemented in order to detect the relevant elements of the images. These images play significant role during the fusion process. In the evaluation phase, a multi-image metric and a quality measure are used in order to represent the percentage enhancements of the fused image[12].

A comparison is carried out with other traditional fusion techniques. We can mention one example here, the standard wavelets approach results improved quality indices as compared to the autofocus and fusion methodology. We can mention here that, the above presented AFA algorithm enhances the image quality in reduced amount of time as compared to other classical approaches. They introduced an advanced multifocus image fusion technique with the help of content adaptive denoising scheme [13]. Multi-focus image fusion has become the most popular research domain because of the information fusion process. It has an objective to enhance the depth-of-field through extraction of focused regions out of multiple partially focused images. All of these regions are combined together in order to generate a composite image. In the above-mentioned composite image, all objects are in focus. In this research paper, a multi-focus image fusion approach is introduced. According to this method, Content Adaptive Blurring (CAB) algorithm is applied which has the responsibility to identify the focused regions. This approach creates non-uniform noise in case of a multi-focus image according to the underlying content. We can also say that, it considers the regional image quality in the neighbourhood in order to determine if the noise should be induced or not. The image quality is not hampered here. Each and every pixel of noisy regions have very little or no noise. But, all of the focused regions have significant noise. An initial segmentation map is generated through evaluating the absolute difference of the original image and the CAB-noisy image. Morphological operators play a vital role during the refinement process. Apart from this, graph-cut approaches are essential to enhance the overall segmentation accuracy.

In the paper [14], authors developed a new multi-scale image fusion approach with the help of rolling guidance filter. Image fusion approach is considered as the most important approach in improvising the visual quality through blending of complementary images. These above complementary images are generated from various constraints or sensors in a particular scenario. The applications of image fusion approaches are increasing day by day. All data gathered through multiple visual sensors require additional computation or fusion. The additional computation or fusion completely depends upon a network of decision making or analysis. In this research paper, an advanced image fusion approach is introduced with the help of rolling guidance filter and joint bilateral filter. Initially, the saliency maps of two numbers of images are extracted and gathered with the help of Kirsch operator. In the subsequent phase, both of the source images are spilt with the help of rolling guidance filter. Rolling guidance filter has the responsibility to generate multi-scale images. Additionally, joint bilateral filter and optimal correction are used to optimize the saliency maps and it also produces the resultant weight maps. At last, two numbers of fusion rules are required during the restoration process of final fused image. The above presented approach preserves every individual detail of source images. Apart from this, it also suppresses the artifacts. By analysing the outcomes of this approach, we can state here that, it is better as compared to all other traditional approaches. Different wavelet-based techniques use wavelets to turn the data into a different base, where "large" coefficients correspond to the signal, and "small" ones mostly reflect noise. Denounced data is obtained by converting the threshold or shrunk coefficients correctly in reverse. Two dimensional variants of methods were introduced with that originally developed for one-dimensional signals and contrasted with the proposed method for images.

Many picture denouncing algorithms, as stated in the literature, showed superior performance under low noise. And their output degrades under high noise[15]. Additionally, wavelet-based, contourlet-based image denotation techniques have less simple directional geometry and are unable to reflect sharp transitions or singularities. The basic functions used for transforming domain methods are constant and thus it is difficult to distinguish natural images with different patterns. Sparse representation based on synthesis has a greater computational complexity[16]. We are therefore inspired to explore and improve successful denotion strategies for reducing noise from highly corrupted images.

Gaussian filter reduces noise by attenuating high frequencies in a noisy image. However, it smooths sharp image features such as texture and edges . Anisotropic filter [16] smooths the image along the direction that is orthogonal to the direction of

gradient. Due to this property, anisotropic filter preserves corners and junctions during the filtering process.

**PROPOSED MODEL**

The main objective of this paper is to predict the noise from themedical noisy images in order to minimize the mean squared error rate. Proposed technique is used to decompose the input image into frequency sub-levels knowns as bands. Here, each band is filtering using the proposed thresholding based denosing method to reconstruct the image from the noisy image as shown in figure 3. As shown in fig 4, input data is represented as x variable and noise is added to the input data x in the first layer of auto encoder CNN framework. In the middle layers known as hidden layers, proposed denoising approach is applied on the noisy data to reconstruct the original noiseless image as output.

The layer by layer view of proposed autoencoders based CNN framework is represented in figure 4. As shown in fig 5, two encoders and two decoders are used to denoise the medical image using the proposed compressive sensing based thresholding approach.

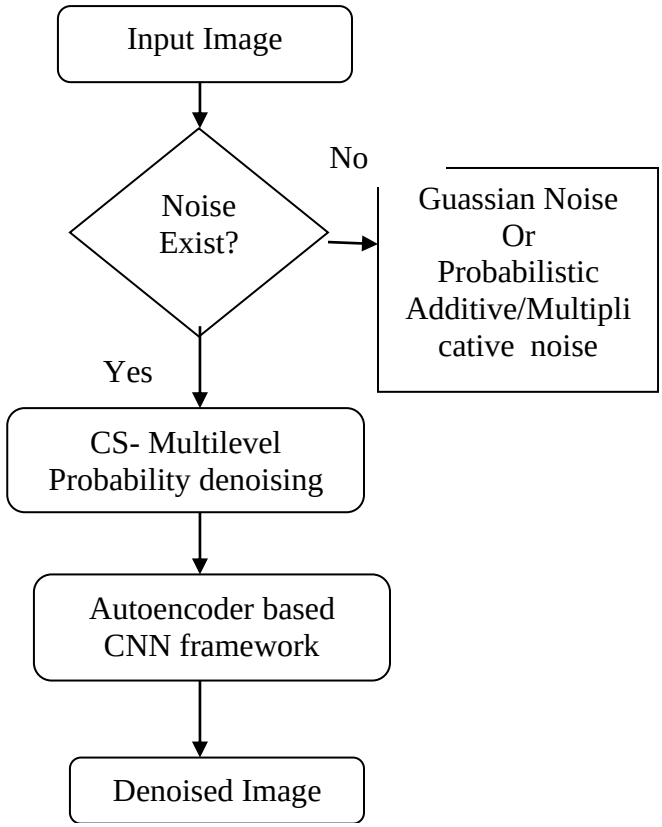


**Figure 3: Overview of Proposed Model**

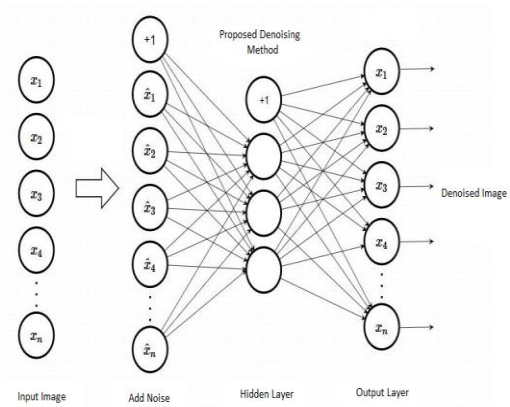


**Figure 4: CNN framework architecture for image denoising**

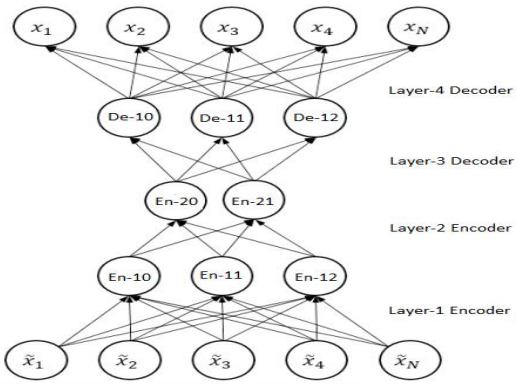


**Figure 5: Layer by layer view of autoencoding and deconding process in CNN framework.**

**Compressive Sensing based Multilevel Denoising Approach(**CS-MLD)
Proposedapproach is used to denoise the input image signal using compressive sensing based on entropy transformation measure.

**Compressive Sensing based Multilevel Denoising Approach(**CS-MLD)
Proposed approach is used to denoise the input image signal using compressive sensing based on entropy transformation measure.
Speckle noise is a multiplicative noise represented mathematically as

$$G(x,y) = F(x,y) * N(x,y)$$

Where 'G' is the degraded image, 'F' represents the radar scattering of ground targets and 'N' represents the speckle noise. The coefficients obtained after the transform domain can be represented as

$$G_{i,j} = F_{i,j} + N_{i,j}$$

Where 'i' represents the scale and 'j' represents the direction. In order to calculate the adaptive threshold first it is necessary to estimate the noise variance and the noise variance of the above mathematical expression can be represented as

$$\sigma_G^2 = \sigma_F^2 + \sigma_N^2$$

Using median absolute deviation (MAD) noise variance can be estimated as :

$$\eta(i,j) = \frac{i^2 + j^2 - 2*\sigma_G^2}{\sigma_G^4}.e^{-\frac{(i^2+j^2)}{2.\sigma_G^2}}$$

$$\hat{\sigma}_N = \frac{median(|G_{i,j}|)}{\min\{0.6745,\ \eta(i,j)/N\}}$$

The mutual information measure is used to find the essential key noise information in each CNN layer. The basic computational measure of MI is given as

$$\text{MI(I):} -p_i \sum_{i=1}^{m} \tau.l\,\text{og}\sqrt[n]{p_i}$$

Where $p_i$ represents the probability of each noise and noiseless region predictor and $\tau$ is the normalized scaling factor.

Let $N = \sum_{i=1}^{\rho} f_i$ represents the frequency of the ith level block pixels count.

The correlation estimator of the ith CNN layer is computed as

$$\text{Prob}_i = \frac{f_i}{N}; \text{Prob}_i > 0, \sum \text{Prob}_i = 1$$

Each probability based block region is given to CNN layered structure for noise processing.

$$M_1(x,y) = (Th.\nabla(G_{min}(x,y)) + |\sigma_X(I-\mu_1)|)$$
$$M_2(x,y) = (Th.\nabla(G_{max}(x,y)) + |\sigma_X(I-\mu_2)|)$$

$$wm_k = \sum_{i \in s_k} P_i$$

$$\eta = \sum_{i \in s_k} \frac{P_i.\max\{i, g*\log(i)\}}{wm_k}; g \in (0,1)$$

The weighted noisy features extracted in the hidden layers for autoencoding process is given $G_{min}(x,y)$ and $G_{max}(x,y)$. Here, the minimum and maximum gaussian metric is used to find the depth of noise in each level of the image. The weighted level wise noise is computed as

$$G_{min}(x,y) = min\{\frac{e^{-\sqrt{x^2+y^2}/2.\sigma_X^2}}{\sigma_X\sqrt{2.\pi}}, \frac{e^{-\sqrt{x^2+y^2}/2.\sigma_y^2}}{\sigma_y\sqrt{2.\pi}}\}$$

$$G_{max}(x,y) = max\{\frac{e^{-\sqrt{x^2+y^2}/2.\sigma_X^2}}{\sigma_X\sqrt{2.\pi}}, \frac{e^{-\sqrt{x^2+y^2}/2.\sigma_y^2}}{\sigma_y\sqrt{2.\pi}}\}$$

$$\mu_{WI} = \sum_{i=0}^{\rho} i * P_i$$

$$\sigma_{VS}^2 = (\sum_{i=0}^{\rho} ws_k.\eta^2 - \mu^2{}_{WI}) / \{G_{min}(x,y) + G_{max}(x,y)\}$$

$$(\sigma_{VS}^2)^* = \sum \max\{M_1(x,y).\sigma_{VS}^2(S_i), M_2(x,y)\sigma_{VS}^2(S_j)\}$$

The weighted threshold for image reconstruction process is given as

$$I_R = (\mu_{WI}) \frac{\sigma_{VS}^2}{\sqrt{\text{Max}(\sigma_{VS}^2 - (\sigma_{VS}^2)^*, 0)}}$$

$$\min\{K(x)\} = \frac{1}{2} \| \sigma_{VS}^2 - (\sigma_{VS}^2)^* \|^2 + I_R.\mu_{WI}$$

Here, K(x), here input noisy image is restored with high PSNR ratio and low error rate.

**EXPERIMENTAL RESULTS**
In this section, we assess the different medical noise images such as MRI ,CT scan and thermal images are used to check the performance of our proposed method in CNN model. We compare the performance of our method with different denoising approaches with CNN framework . For visual and quantitative performance, we consider two criteria which include PSNR and SSIM . The image PSNR ratios are used to verify the performance of the proposed model in the existing image reconstruction models. For the analysis of performance, measurements are selected by undersampling of space via compressive sensing. In the experimental study, the PSNR and structural similarity index measures are used. The PSNR measures the quality of the restored image as compared to the original image and contains a mean square error of the reconstructed image. Simulated results are achieved using 256x256 standard medical grayscale images at various compression levels and multiplying noise at different noise levels.

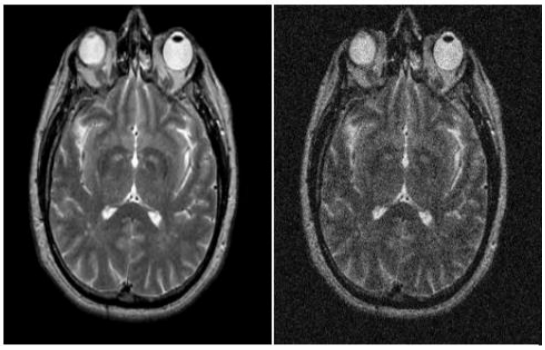

**Figure 6) Input noisy image**

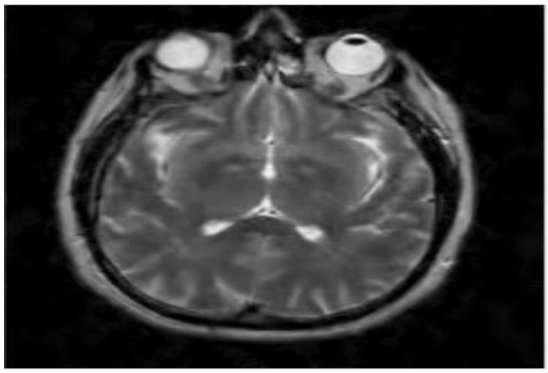

**Figure 7) Filtered denoisy image**

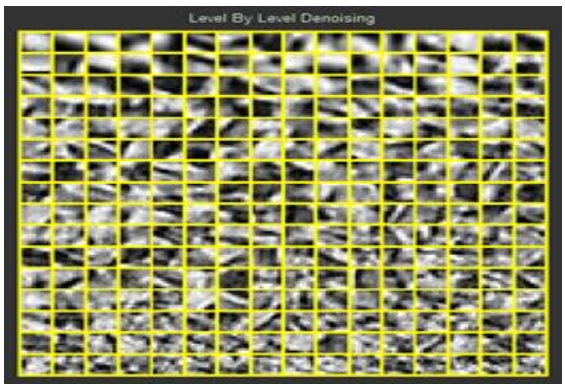


**Figure 8: level by level CNN Thresholding for image denoising**.

**Experiment 2:**

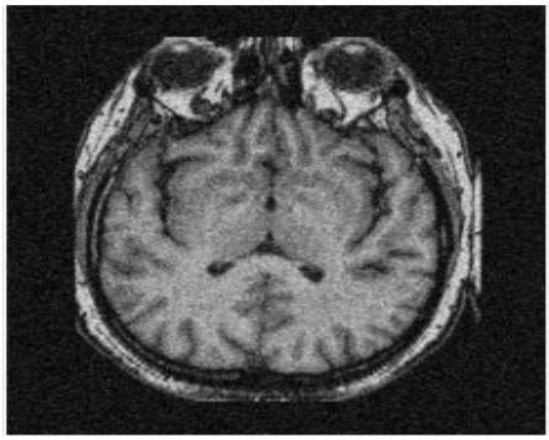

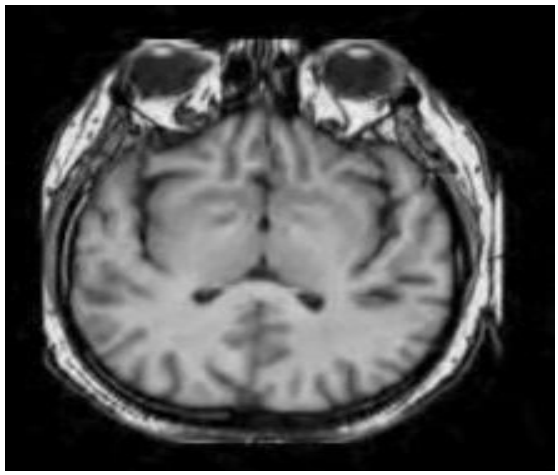

Figure 9: a) Noise image b) Restored image .
Figure 9, describes the improvement of the proposed model for image restoring. From the figure, it is clearly observed that the proposed model has high PSNR ratio compared to the noise image with different levels of noise levels.

**Experiment 3:**

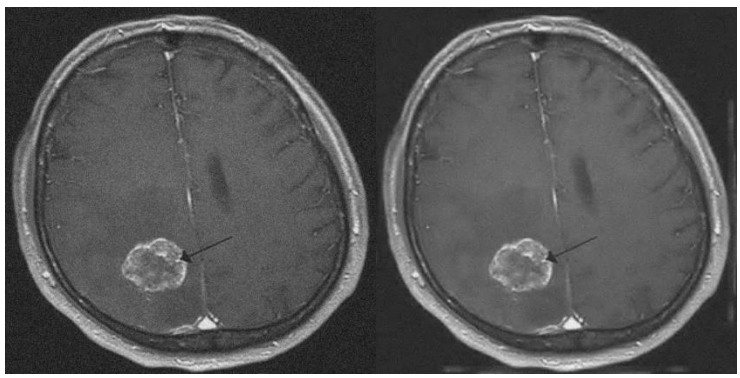

**Figure 10: a) Noisy brain tumor image b) Restored image .**

Figure 12, describes the improvement of the proposed model for image restoring. From the figure, it is clearly observed that the CS-MLD model has high PSNR ratio compared to the noise image with different levels of noise levels.

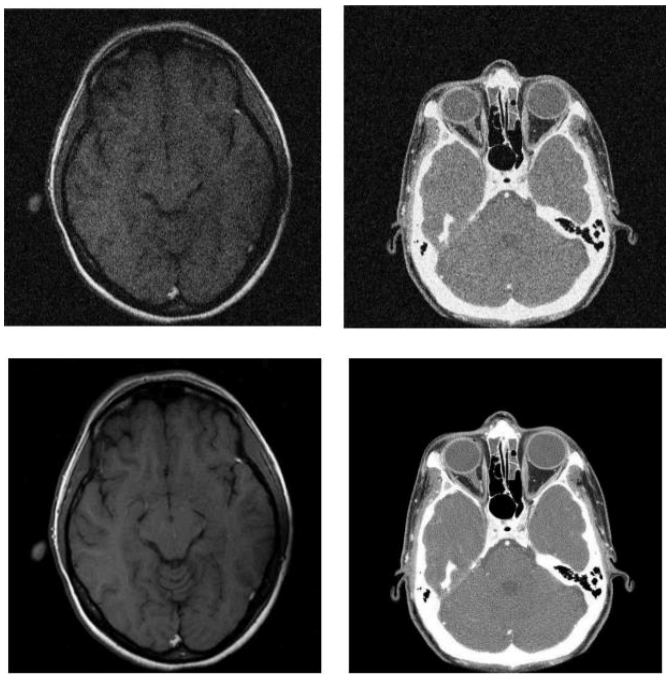

**Table 1: Comparative analysis of proposed model to the traditional techniques in terms of average PSNR ratio for all images with different levels of noise levels.**

| Noise Levels(%) | DWT+CNN | Bayesian+CNN | WDWT+CNN | PCA+CNN | PROPOSED |
|---|---|---|---|---|---|
| #10 | 25.74 | 24.57 | 27.35 | 28.56 | 32.35 |
| #20 | 23.76 | 25.45 | 27.76 | 30.62 | 31.86 |
| #30 | 24.53 | 26.83 | 29.47 | 32.67 | 34.24 |
| #40 | 22.56 | 24.86 | 26.88 | 29.45 | 30.87 |
| #50 | 24.76 | 27.34 | 28.13 | 29.14 | 32.03 |

Table 1 describes the comparative analysis of present technique to the traditional techniques using average PSNR ratio of all input images. From the table-1 it is clearly observed that the CS-MLD technique has high computational PSNR efficiency compared to the existing techniques.

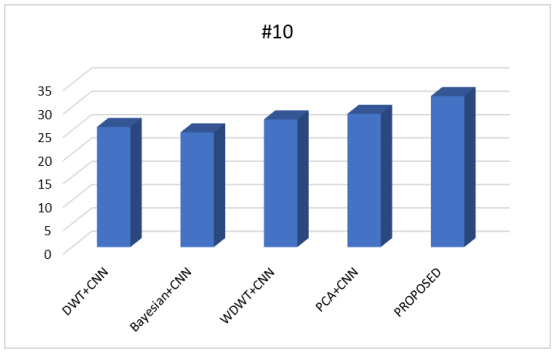


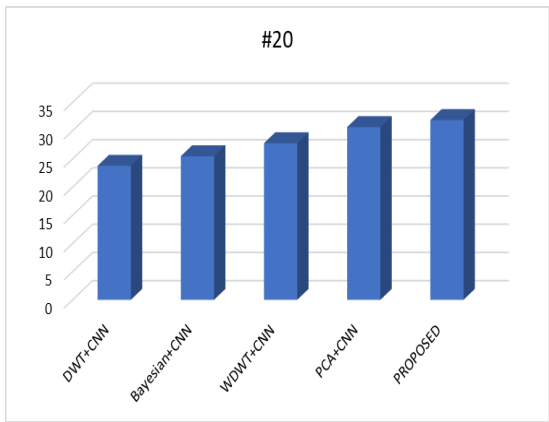

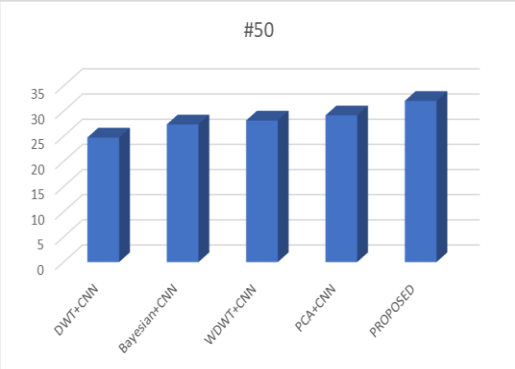


**Figure 11: Graphical comparison of Avg PSNR ratio of proposed model to the existing models for noise % levels 10,20,50.**

## CONCLUSION

Compressive sensing has the potential to generate optimal image restoring process in lower bandwight imaging systems.Most of the compressed or noisy images are difficult to analyze using the traditional denosing methods such as non-linear median filter, Bayesian filter, wavelt based shearlet transform etc, due to the existence of noise on the edges. Also, traditional image reconstruction model cannot solve the problem of sparsity in different still or compressed images. To overcome these issues, a novelcompressive sensing based multilevel denoising technique is proposed to minimize the noise rate of medical images in the Convolution neural network(CNN) framework. This technique is implemented in convolutional autoencoders framework to reduce the noise in each deep network layer and to improve the quality of the images. This technique efficiently denoise the medical images using the inter, intra variance in the CNN framework. Experimental results demonstrated that the proposed framework has better PSNR and SSIM measures compared to the traditional state-of-the-art approaches.

## REFERENCES

1. G. Andria, F. Attivissimo, G. Cavone, N. Giaquinto, and A. M. L. Lanzolla, “Linear filtering of 2-D wavelet coefficients for denoising ultrasound medical images,” Measurement, vol. 45, no. 7, pp. 1792–1800, Aug. 2012, doi: 10.1016/j.measurement.2012.04.005.
2. M. Elhoseny and K. Shankar, “Optimal bilateral filter and Convolutional Neural Network based denoising method of medical image measurements,” Measurement, vol. 143, pp. 125–135, Sep. 2019, doi: 10.1016/j.measurement.2019.04.072.
3. S. Lee et al., “Noise removal in medical mammography images using fast non-local means denoising algorithm for early breast cancer detection: a phantom study,” Optik, vol. 180, pp. 569–575, Feb. 2019, doi: 10.1016/j.ijleo.2018.11.167.
4. H. Li, X. He, D. Tao, Y. Tang, and R. Wang, “Joint medical image fusion, denoising and enhancement via discriminative low-rank sparse dictionaries learning,” Pattern Recognition, vol. 79, pp. 130–146, Jul. 2018, doi: 10.1016/j.patcog.2018.02.005.
5. X. Mingliang et al., “Medical image denoising by parallel non-local means,” Neurocomputing, vol. 195, pp. 117–122, Jun. 2016, doi: 10.1016/j.neucom.2015.08.117.
6. A. Miri, S. Sharifian, S. Rashidi, and M. Ghods, “Medical image denoising based on 2D discrete cosine transform via ant colony optimization,” Optik, vol. 156, pp. 938–948, Mar. 2018, doi: 10.1016/j.ijleo.2017.12.074.
7. Garg, R. Vijay, and S. Urooj, “Statistical Approach to Compare Image Denoising Techniques in Medical MR Images,” Procedia Computer Science, vol. 152, pp. 367–374, Jan. 2019, doi: 10.1016/j.procs.2019.05.004.
8. P. Görgel and A. Simsek, “Face recognition via Deep Stacked Denoising Sparse Autoencoders (DSDSA),” Applied Mathematics and Computation, vol. 355, pp. 325–342, Aug. 2019, doi: 10.1016/j.amc.2019.02.071.
9. B. Goyal, A. Dogra, S. Agrawal, B. S. Sohi, and A. Sharma, “Image denoising review: From classical to state-of-the-art approaches,” Information Fusion, vol. 55, pp. 220–244, Mar. 2020, doi: 10.1016/j.inffus.2019.09.003.
10. Đ. T. Grozdić, S. T. Jovičić, and M. Subotić, “Whispered speech recognition using deep denoising autoencoder,” Engineering Applications of Artificial Intelligence, vol. 59, pp. 15–22, Mar. 2017, doi: 10.1016/j.engappai.2016.12.012.
11. P. Liu, M. D. El Basha, Y. Li, Y. Xiao, P. C. Sanelli, and R. Fang, “Deep Evolutionary Networks with Expedited Genetic Algorithms for Medical Image Denoising,” Medical Image Analysis, vol. 54, pp. 306–315, May 2019, doi: 10.1016/j.media.2019.03.004.
12. H.-J. Kim and D. Lee, “Image denoising with conditional generative adversarial networks (CGAN) in low dose chest images,” Nuclear Instruments and Methods in Physics Research Section A: Accelerators, Spectrometers, Detectors and Associated Equipment, vol. 954, p. 161914, Feb. 2020, doi: 10.1016/j.nima.2019.02.041.
13. P. V. V. Kishore, K. L. Mallika, M. V. D. Prasad, and K. L. Narayana, “Denoising Ultrasound Medical Images with Selective Fusion in Wavelet Domain,” Procedia Computer Science, vol. 58, pp. 129–139, Jan. 2015, doi: 10.1016/j.procs.2015.08.040.
14. R. Lan, Z. Li, Z. Liu, T. Gu, and X. Luo, “Hyperspectral image classification using k-sparse denoising autoencoder and spectral–restricted spatial characteristics,” Applied Soft Computing, vol. 74, pp. 693–708, Jan. 2019, doi: 10.1016/j.asoc.2018.08.049.
15. N. Munir, J. Park, H.-J. Kim, S.-J. Song, and S.-S. Kang, “Performance enhancement of convolutional neural network for ultrasonic flaw classification by adopting autoencoder,” NDT & E International, p. 102218, Jan. 2020, doi: 10.1016/j.ndteint.2020.102218.
16. H. Naimi, A. B. H. Adamou-Mitiche, and L. Mitiche, “Medical image denoising using dual tree complex thresholding wavelet transform and Wiener filter,” Journal of King Saud University - Computer and Information Sciences, vol. 27, no. 1, pp. 40–45, Jan. 2015, doi: 10.1016/j.jksuci.2014.03.015.
17. Kalaivani Selvaraj, Girija Sivakumar, Vishnu Priya Veeraraghavan, Vijaya S Dandannavar, Geetha Royapuram Veeraraghavan, Gayathri Rengasamy. "Asparagus Racemosus - A Review." Systematic Reviews in Pharmacy 10.1 (2019), 87-89. Print. doi:10.5530/srp.2019.1.14